Vortex Locking in Direct Numerical Simulations of Quantum Turbulence

Karla Morris,[1] Joel Koplik,[2,3] and Damian W. I. Rouson[4]

[1]*Department of Mechanical Engineering, City College of the City University of New York, New York, New York 10031, USA*
[2]*Benjamin Levich Institute, City College of the City University of New York, New York, New York 10031, USA*
[3]*Department of Physics, City College of the City University of New York, New York, New York 10031, USA*
[4]*Scalable Computing Research and Development Department, Sandia National Laboratories, Livermore, California 94550, USA*

(Received 28 February 2008; revised manuscript received 21 April 2008; published 3 July 2008)

Direct numerical simulations are used to examine the locking of quantized superfluid vortices and normal fluid vorticity in evolving turbulent flows. The superfluid is driven by the normal fluid, which undergoes either a decaying Taylor-Green flow or a linearly forced homogeneous isotropic turbulent flow, although the back reaction of the superfluid on the normal fluid flow is omitted. Using correlation functions and wavelet transforms, we present numerical and visual evidence for vortex locking on length scales above the intervortex spacing.

DOI: 10.1103/PhysRevLett.101.015301 PACS numbers: 67.25.dk, 67.25.dm

A growing body of empirical evidence suggests that the macroscopic statistical behavior of quantum turbulence closely matches that of classical turbulence despite considerable differences in the physics at the mesoscopic scale of the intervortex spacing and the microscopic scale of the vortex core diameters [1–3]. Although a commonly used phenomenology involving quantum-vortex/normal-vortex locking has achieved some success in explaining the macroscopic similarities, current laboratory measurements lack sufficient spatial resolution to verify vortex locking. We therefore turn to numerical simulations to confirm the existence and explore the limitations of this phenomenology. Previous numerical simulations have considered the special case of a superfluid in the presence of a static normal fluid flow field. Barenghi *et. al.* [4] utilized an idealized normal fluid turbulent field based on vorticity tubes, which drove a superfluid vortex ring. In the presence of mutual friction and vortex wave instabilities, the flow evolved into a vortex tangle with a higher filament density and a configuration exhibiting a clear alignment of the superfluid vortex filaments along the normal fluid vortices. Kivotides [5] found similar results using a different driving force for the superfluid, based on a snapshot of a statistically isotropic and homogeneous turbulent state held constant in time while the superfluid was allowed to evolve. In this work, we consider a more realistic situation in which coupled time-dependent normal fluid and superfluid components evolve simultaneously.

Our results are obtained from a direct numerical simulation (DNS) of the dynamics of a one-way coupling between normal fluid and superfluid, in which the superfluid reacts to the normal fluid due to the effects of mutual friction, but the back reaction of the superfluid on the normal fluid is omitted. A fully coupled calculation would involve severe computational difficulties due to the huge disparity in length scales between the superfluid vortex core size and the numerical resolution of any feasible normal fluid turbulence calculation. Fully coupled calculations have only been performed for very simple geometries [6,7]. Computations for the normal fluid component are generated by a DNS of the Navier-Stokes equations. For the superfluid, we adapt methods developed by Schwarz [8] and use parameter values taken from measurements of He^4 at a temperature below the lambda point. The governing equations for the superfluid are based on the two-fluid model of Tisza and Landau [9,10],

$$\boldsymbol{\nabla}\cdot\mathbf{u}_n = 0, \qquad \frac{\partial \mathbf{u}_n}{\partial t} + \mathbf{u}_n\cdot\boldsymbol{\nabla}\mathbf{u}_n = -\frac{1}{\rho}\boldsymbol{\nabla}P + \nu_n\nabla^2\mathbf{u}_n. \tag{1}$$

$$\frac{d\mathbf{s}}{dt} = \mathbf{u}_i + \alpha\mathbf{s}'\otimes(\mathbf{u}_n - \mathbf{u}_i) - \alpha'\mathbf{s}'\otimes[\mathbf{s}'\otimes(\mathbf{u}_n - \mathbf{u}_i)], \tag{2}$$

where $\mathbf{u}_n$ is the velocity of the normal fluid component, $\mathbf{u}_i$ is the induced velocity on a vortex filament. The filament itself is parametrized as $\mathbf{s}(\xi, t)$, where ξ is the arclength and t is the time, $\mathbf{s}' = d\mathbf{s}/d\xi$, and α and α' are mutual friction coefficients which depend on the temperature of the fluid. The induced velocity $\mathbf{u}_i$ is calculated using the Biot-Savart law, and the singularity in the latter when source and observation points nearly coincide is dealt with by separating the integral into local and nonlocal contributions [8,9]. The superfluid vortex filaments are remeshed at each time step in the simulation to maintain a near-constant spacing between grid points, to provide an accurate representation of the filaments as they stretch and transform their shape. When two vortex filaments intersect, they are reconnected provided the total vortex line length decreases [9,11], a rule motivated by the connection between energy and vortex line length. During the reconnection of two intersecting superfluid vortex filaments sound energy is released which leads to a loss of vortex line length [12]. This transfer of energy within the turbulent

vortex tangle has also been related to the radiation of Kelvin waves [13].

The first case considered here involves an evolving Taylor-Green flow with no forcing, so the flow dies out over time. During an intermediate interval within this process, the flow attains a quasisteady state condition characterized by a nearly constant Taylor microscale Reynolds number. The Taylor-Green flow has been used previously to study the generation of small energy scales from large ones in classical turbulence [14,15]. In the current case, the DNS was carried out at a temperature of $T = 2.1$ K with the following fluid properties: quantum of circulation $\kappa = 9.97 \times 10^{-4}$ cm^2/s, core radius $a_0 = 10^{-8}$ cm, $\alpha = 0.498$, $\alpha' = -0.030$, and $\rho_n/\rho = 0.749$ where ρ_n is the density of the normal fluid component and ρ is the density of He II at the working temperature [2,16]. The DNS of the normal fluid component is performed on a grid of 256^3 points, and its initial condition takes the form $\mathbf{u}_n = \sin(x)\cos(y)\cos(z)\mathbf{i} - \cos(x) \times \sin(y)\cos(z)\mathbf{j} + 0\mathbf{k}$. The initial configuration for the superfluid component is a collection of 10 identical rings randomly oriented, with a radius of 0.159 cm. Results as the flow commences its decay at $t = 24.1$ s are shown in Fig. 1, indicating the obvious visual similarity of the superfluid and normal fluid vorticity fields.

To quantify the relationship between the two components and assess the degree of vortex locking, we define a vorticity correlation coefficient for the normal fluid and superfluid components as

$$r = \frac{\langle w_s w_n \rangle}{\sqrt{\langle w_s{}^2 \rangle \langle w_n{}^2 \rangle}}, \tag{3}$$

where w_n and w_s are either the magnitudes or individual vector components of the normal fluid and superfluid vorticity, respectively. The computational box which has a size of 1 cm in every direction is divided into cells of variable size to compute the correlation coefficient as a spatially averaged function of length scale. Since the vorticity of the superfluid component is confined to the vortex filaments the total superfluid vorticity of a cell is calculated by summing the contributions of the filaments within it. For the normal fluid component, the vorticity field is first denoised via wavelet transforms to extract the coherent vortex structures [17], the total vorticity of the cells is then inserted in (3). Figure 2(a) depicts the evolution over time of the correlation coefficient, which shows temporally increasing correlations for both the magnitude and the direction of the vorticity. The growth of the correlations with time indicates that the superfluid filaments become increasingly locked to the normal fluid vorticity. To explore the degree of correlation as a function of length scale we calculate the various correlations r_i for the vorticity (w_n and w_s) within cubic cells of linear size Δ. The numerical analysis was done after the aforementioned quasisteady state was reached, when decay starts at $t = 24.1$ s and the results are plotted in Fig. 2(b). We see that the correlations are weak for small cell size but grow roughly as $\sqrt{\Delta}$, and, in particular, become quite strong once Δ exceeds the average intervortex spacing $\delta \approx 0.308$. (We estimate δ from the total vortex line length L and simulation box volume V as $\delta = \sqrt{V/L}$ and is given relative to the box size.) For the normal fluid component the Kolmogorov length scale at $t = 24.1$ s is $\eta = 0.031$ cm when calculated based on $\eta = l\mathrm{Re}^{-3/4}$ where l is half the computational box size and $\mathrm{Re} = (u_{\mathrm{rms}} l/\nu_n) = (u_{\mathrm{rms}} l \rho_n/\mu)$. Next we consider superfluid coupled to a normal fluid in a statistically homogeneous and isotropic turbulent flow maintained by linear forcing at a Taylor microscale Reynolds number of 42 [18,19]. The governing equation for the normal fluid component is the forced Navier-Stokes equation

$$\frac{\partial \mathbf{u}_n}{\partial t} + \mathbf{u}_n \cdot \boldsymbol{\nabla} \mathbf{u}_n = -\frac{1}{\rho}\boldsymbol{\nabla} P + \nu_n \nabla^2 \mathbf{u}_n + \mathbf{F} \tag{4}$$

where the forcing term $\mathbf{F} = A\mathbf{u}_n \equiv (\varepsilon/3u_{\mathrm{rms}}^2)\mathbf{u}_n$ is related to the energy dissipation rate $\varepsilon = -\nu_n \langle \mathbf{u}_n \cdot \nabla^2 \mathbf{u}_n \rangle$ and the

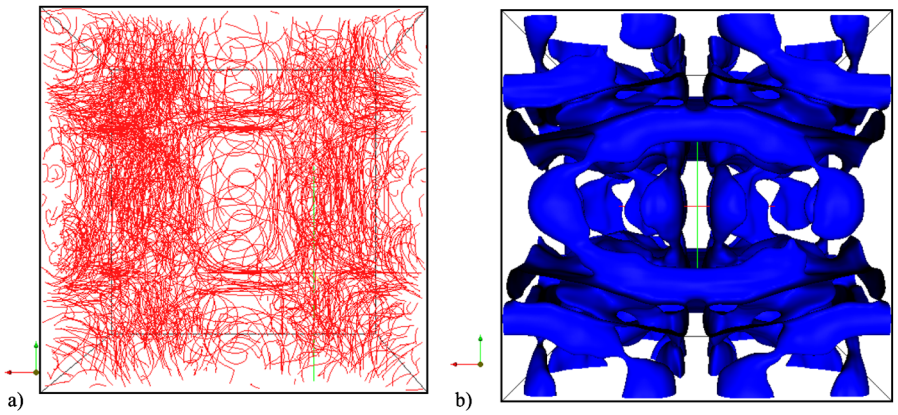

FIG. 1 (color online). Vorticity plots of Taylor-Green flow for He II at $T = 2.1$ K, and $t = 24.1$ s. (a) Superfluid vortex filaments. (b) Normal fluid vorticity isosurface.

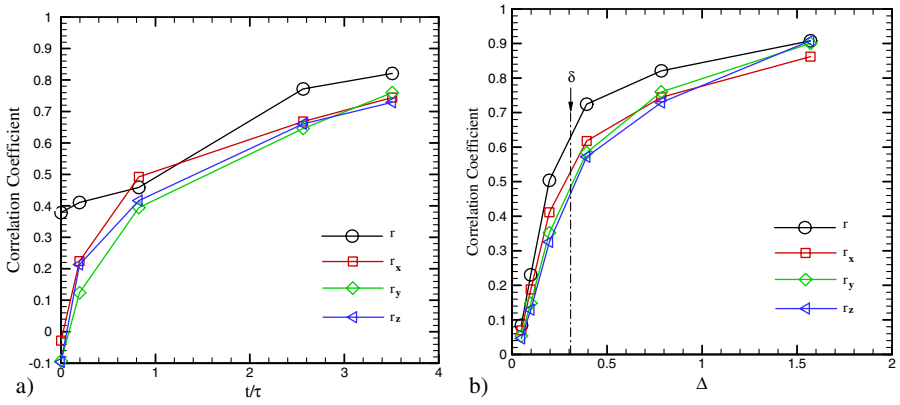

FIG. 2 (color online). Vorticity correlations for the Taylor-Green flow in He^4 at 2.1 K. (a) Time evolution of the correlation coefficients of superfluid and normal fluid vorticity; r is the correlation coefficient for the vorticity magnitude and $r_{x,y,z}$ are the coefficients for individual vector components. The vorticity is computed for a cell size $\Delta = 0.785$. (b) Length scale dependence of the correlation coefficients in decaying Taylor-Green flow ($t = 24.1$ s): Δ is the cell size and δ is the average intervortex spacing (Δ and δ are given relative to the simulation box size).

rms velocity $u_{\mathrm{rms}}^2 = \langle \mathbf{u}_n \cdot \mathbf{u}_n \rangle / 3$. In this case we allow the normal fluid to reach a statistically stationary state before introducing the superfluid component. The superfluid initial configuration is the same as in the Taylor-Green flow—a random collection of vortex rings. The simulation here was done at a temperature of $T = 2.1$ K with the same fluid properties as previously stated. For the normal fluid the dimensionless viscosity is $\nu = 4.491 \times 10^{-3}$ and the forcing coefficient is $A = 0.1333$. The initial vortex line length in this flow is $L_0 = 9.98$ cm and during the simulation as the energy of the normal fluid component is transferred to the superfluid component the vortex length grows to $L_f = 1533$ cm. In the final configuration the average vortex spacing for the superfluid tangle is $\delta = 0.16$ (given relative to box size) while in the normal fluid component the Kolmogorov length scale is $\eta = 0.007$ cm. An example of direct visualization of vortex locking is given in Fig. 3, which shows a cut through the computational box at $t = 5.65$ s. While there is certainly some apparent similarity in the two figures, because of the high vortex line density and the increased randomness of this flow, vortex locking is not as visually obvious as in the previous case. However, a numerical analysis of correlations similar to the one done in the Taylor-Green case confirms locking of the vortices.

The time evolution of the correlation coefficients in this case is similar to that shown in Fig. 2(a), and as before we find a monotonic increase in the vorticity correlation over time. To analyze our final configuration we again consider the correlation of vorticity as a function of cell size Δ. In Fig. 4(a) we see that the correlation is large when the vorticity is calculated over a length scale larger than the average vortex line spacing. A direct visualization of this correlation in cells of size $\Delta = 1.571$ is given in Fig. 4(b), and provides a more local indication of vortex locking.

In summary, by performing a DNS of a turbulent helium flow, we were able to confirm previous conjectures regarding the experimentally observed similarities in the macroscopic statistics of classical and quantum turbulence. In the one-way coupled evolution, the superfluid component absorbs energy from the normal fluid component, and as a result of mutual friction and vortex wave instabilities, a highly dense vortex tangle develops, wherein the superfluid vortex filaments align with the normal fluid vorticity. This

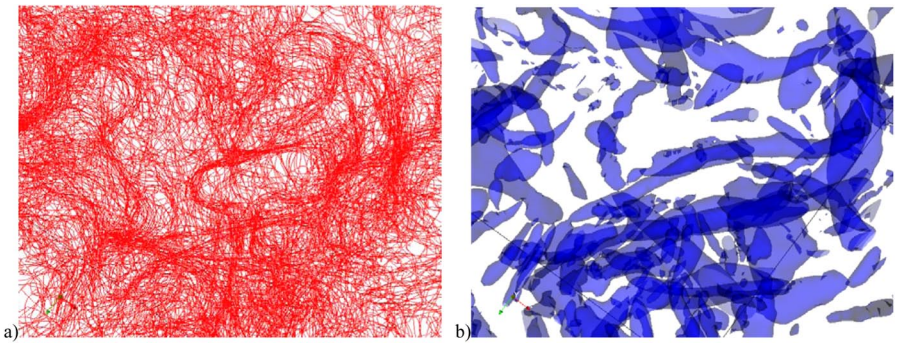

FIG. 3 (color online). Forced homogeneous isotropic turbulence flow in He^4 at a temperature of 2.1 K at $t = 5.65$ s. (a) Superfluid vortex filaments. (b) Normal fluid vorticity isosurface.

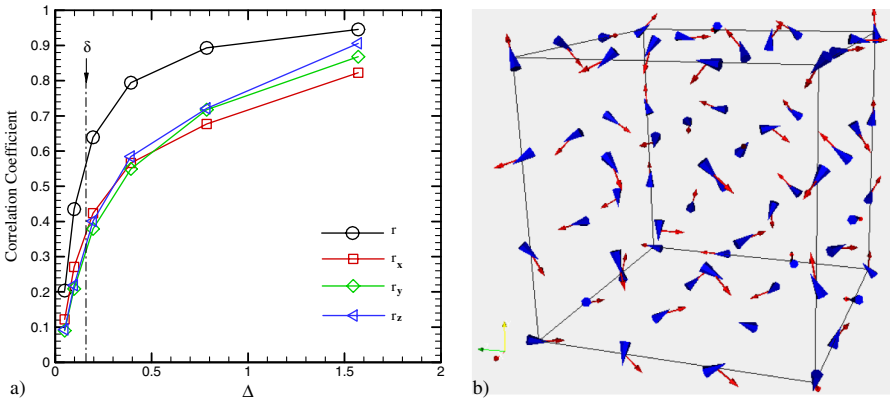

FIG. 4 (color online). Vorticity correlations in forced isotropic turbulence flow in He^4 at a temperature of 2.1 K at $t = 5.65$ s. (a) Correlation coefficient of superfluid and normal fluid vorticity as a function of cell size (Δ and δ are given relative to the simulation box size). (b) Vorticity vectors for superfluid vortex filaments (arrows) and normal fluid (cones) at $t = 5.65$ s.

alignment has been shown to be a direct consequence of Eq. (2) according to which the superfluid vortex lines are polarized by the normal fluid eddies [20]. Once this alignment, or locking, of quantum vortices and classical vortices has occurred, both components follow a similar motion. This was directly observed for a linearly forced, isotropic turbulent flow where the similarities between superfluid and normal fluid components increased as the flow evolved. These statistical similarities are most pronounced for length scales that are large compared to intervortex spacing.

This work was supported in part by the NSF/CREST Center for Mesoscopic Modeling and Simulation at CCNY, and NSF/AGEP No. HRD 0450360.

[1] Y. S. Choi, M. R. Smith, and S. W. Van Sciver, in *Quantized Vortex Dynamics and Superfluid Turbulence*, edited by C. F. Barenghi, R. J. Donnelly, and W. F. Vinen, Lectures Notes in Physics (Springer, New York, 2001).
[2] W. F. Vinen and J. J. Niemela, J. Low Temp. Phys. **128**, 167 (2002).
[3] S. R. Stalp, J. J. Niemela, W. F. Vinen, and R. J. Donnelly, Phys. Fluids **14**, 1377 (2002).
[4] C. F. Barenghi, D. Samuels, G. H. Bauer, and R. J. Donnelly, Phys. Fluids **9**, 2631 (1997).
[5] D. Kivotides, Phys. Rev. Lett. **96**, 175301 (2006).
[6] D. Kivotides, C. F. Barenghi, and D. C. Samuels, Europhys. Lett. **54**, 774 (2001).
[7] D. Kivotides, C. F. Barenghi, and D. C. Samuels, Science **290**, 777 (2000).
[8] K. W. Schwarz, Phys. Rev. B **31**, 5782 (1985).
[9] D. Samuels, in *Quantized Vortex Dynamics and Superfluid Turbulence*, edited by C. F. Barenghi, R. J. Donnelly, and W. F. Vinen, Lectures Notes in Physics (Springer, New York, 2001).
[10] C. F. Barenghi, in *Quantized Vortex Dynamics and Superfluid Turbulence*, edited by C. F. Barenghi, R. J. Donnelly, and W. F. Vinen, Lectures Notes in Physics (Springer, New York, 2001).
[11] J. Koplik and H. Levine, Phys. Rev. Lett. **71**, 1375 (1993).
[12] M. Leadbeater, T. Winiecki, D. C. Samules, C. F. Barenghi, and C. S. Adams, Phys. Rev. Lett. **86**, 1410 (2001).
[13] D. Kivotides, J. C. Vassilicos, D. C. Samuels, and C. F. Barenghi, Phys. Rev. Lett. **86**, 3080 (2001).
[14] G. I. Taylor and A. E. Green, Proc. R. Soc. A **158**, 499 (1937).
[15] M. E. Brachet, D. I. Meiron, S. A. Orszag, B. G. Nickel, R. H. Morf, and U. Frisch, J. Fluid Mech. **130**, 411 (1983).
[16] R. J. Donnelly, *Quantized Vortices in Helium II* (Cambridge University Press, Cambridge, U.K., 1991).
[17] M. Farge, K. Schneider, G. Pellegrino, A. A. Wray, and R. S. Rogallo, Phys. Fluids **15**, 2886 (2003).
[18] C. Rosales and C. Meneveau, Phys. Fluids **17**, 095106 (2005).
[19] T. S. Lundgren, in *Linearly Forced Isotropic Turbulence*, Annual Research Briefs (Center for Turbulence Research, Stanford, 2003), pp. 461–473.
[20] C. F. Barenghi, S. Hulton, and D. C. Samules, Phys. Rev. Lett. **89**, 275301 (2002).